International Journal of Mechanical, Industrial and Aerospace Sciences
ISSN: 2517-9950
Vol:5, No:7, 2011

# A Finite Volume Procedure on Unstructured Meshes for Fluid-Structure Interaction Problems

P I Jagad, B P Puranik, and A W Date

*Abstract*—Flow through micro and mini channels requires relatively high driving pressure due to the large fluid pressure drop through these channels. Consequently the forces acting on the walls of the channel due to the fluid pressure are also large. Due to these forces there are displacement fields set up in the solid substrate containing the channels. If the movement of the substrate is constrained at some points, then stress fields are established in the substrate. On the other hand, if the deformation of the channel shape is sufficiently large then its effect on the fluid flow is important to be calculated. Such coupled fluid-solid systems form a class of problems known as fluid-structure interactions. In the present work a co-located finite volume discretization procedure on unstructured meshes is described for solving fluid-structure interaction type of problems. A linear elastic solid is assumed for which the effect of the channel deformation on the flow is neglected. Thus the governing equations for the fluid and the solid are decoupled and are solved separately. The procedure is validated by solving two benchmark problems, one from fluid mechanics and another from solid mechanics. A fluid-structure interaction problem of flow through a U-shaped channel embedded in a plate is solved.

*Keywords*—Finite volume method, flow induced stresses, fluid-structure interaction, unstructured meshes.

## I. Introduction

WHEN a fluid flows through a channel it exerts forces on the walls of the channel due to its pressure. These forces set up displacement fields in the solid substrate containing the channel. If the movement of substrate is constrained at some points, say by clamping or by screwing, then stress fields are also set up in the substrate. When the pressure of the fluid is high it is important to determine the displacement and the stress fields in the substrate since these may lead to failure of the system. On the other hand if the deformation of the channel due to the fluid pressure forces is sufficiently large then it is important to determine its effect on the fluid flow as well. Such coupled fluid structure systems constitute what are known as fluid-structure interaction type of problems. Some examples of fluid-structure interaction problems include mini and micro channel heat exchangers, electronics cooling, cooling of gas turbine blades, etc.

The finite volume method is of interest due to its suitability for solving the non-linear fluid flow problems. When dealing with fluid-structure interaction type of problems, it is convenient to use for solving the governing equations in the solid as well. There are very few studies found in literature on finite volume methods for fluid-structure interaction type of problems. Demirdzic et al. [1] proposed a numerical method for coupled fluid flow, heat transfer and stress analysis using unstructured moving meshes with cells of arbitrary topology. A finite volume discretization procedure was developed using a co-located grid arrangement. Use of the method was demonstrated by solving a few problems involving fluid-solid coupled situations. Schafer et al. [2] presented a multigrid finite volume method for the prediction of the coupled fluid-solid problems in complex geometries. A unified finite volume approach based on the concept of block structured grid was used for handling the complexity of the geometry and the fluid solid-coupling. To investigate the performance of the method a few problems were solved involving pure solid mechanics as well as coupled fluid-solid situations.

To solve fluid structure-interaction type of problems the governing equations for the fluid and for the solid need to be solved simultaneously. However, within the elastic limit of the solid material usually the effect of the channel deformation on the fluid flow is neglected. Hence the governing equations for the fluid flow and that for the solid can be solved separately. This approach is used in the present work. A co-located finite volume discretization procedure is described for the solution. The flow is considered to be laminar and a linear elastic behavior for the solid is assumed. To validate the procedure two benchmark problems, one from fluid mechanics and another from solid mechanics, are solved. The first problem consists of flow of a fluid over a backward facing step. The second benchmark problem includes a flat plate with a circular hole subjected to a uniform tension. Finally a fluid-structure interaction type of problem is solved. The problem consists of flow of a fluid through a U-shaped channel embedded in a plate. All problems solved in this work assume two-dimensional behavior.

## II. Mathematical formulation and Discretization

The governing transport equations (continuity and momentum) for the fluid as well as for the solid under steady state can be expressed as

$$\frac{\partial (\rho u_j)}{\partial x_j} = 0, \tag{1}$$

and

$$\frac{\partial (\rho u_j u_i)}{\partial x_j} - \frac{\partial \sigma_{ij}}{\partial x_j} = \rho f_i, \tag{2}$$

where $u_j$ is the velocity vector, $\sigma_{ij}$ is the stress tensor, $f_i$ is the resultant body force per unit mass in $i$-direction and $x_j$ is the

P I Jagad is a Research Scholar at the Department of Mechanical Engineering, Indian Institute of Technology Bombay, Mumbai, 400076, India e-mail: 08410003@iitb.ac.in.

B P Puranik and A W Date are with the Department of Mechanical Engineering, Indian Institute of Technology Bombay, Mumbai, 400076, India e-mail:puranik@me.iitb.ac.in, awdate@me.iitb.ac.in.

cartesian coordinate vector. In solids usually the displacement vector is considered as a variable of interest. The velocity vector is expressed in terms of the displacement vector $\delta u_j$ as

$$u_j = \frac{\partial (\delta u_j)}{\partial t}. \tag{3}$$

For the fluid the Stokes' law for a Newtonian fluid is invoked to relate the stress tensor with the rate of strain tensor as

$$\sigma_{ij} = -p\delta_{ij} + 2\mu\varepsilon_{ij} + \delta_{ij}\lambda\varepsilon_{kk}, \tag{4}$$

where $p$ is the pressure, $\delta_{ij}$ is the Kronecker delta, $\mu$ is the coefficient of dynamic viscosity, $\lambda = -\frac{2}{3}\mu$ is the second coefficient of viscosity and $\varepsilon_{ij}$ is the rate of strain tensor. The $\varepsilon_{ij}$ is expressed in terms of the velocity gradients as

$$\varepsilon_{ij} = \frac{1}{2}\left(\frac{\partial u_i}{\partial x_j} + \frac{\partial u_j}{\partial x_i}\right). \tag{5}$$

Invoking the Hooke's law for the solid for relating the stress tensor with the strain tensor, we have

$$\sigma_{ij} = 2\mu\varepsilon_{ij} + \delta_{ij}\lambda\varepsilon_{kk}, \tag{6}$$

where $\mu$ is the shear modulus and $\lambda$ is the Lame's constant. Assuming the material to be homogeneous and isotropic they are expressed as

$$\mu = \frac{E}{2(1+\nu)}, \tag{7}$$

$$\lambda = \frac{\nu E}{(1+\nu)(1-2\nu)}, \tag{8}$$

where $E$ is Young's modulus and $\nu$ is Poisson's ratio.

For small displacements the strain tensor is expressed in terms of displacement gradients as

$$\varepsilon_{ij} = \frac{1}{2}\left(\frac{\partial (\delta u_i)}{\partial x_j} + \frac{\partial (\delta u_j)}{\partial x_i}\right). \tag{9}$$

Introducing the constitutive relations ((4) and (6)) and the kinematic relations ((5) and (9)) into the momentum equations, i.e., into (2), we get

$$\frac{\partial (\rho u_j u_i)}{\partial x_j} - \frac{\partial}{\partial x_j}\left[-p\delta_{ij} + \mu\left(\frac{\partial u_i}{\partial x_j} + \frac{\partial u_j}{\partial x_i}\right) + \lambda\delta_{ij}\frac{\partial u_k}{\partial x_k}\right] = \rho f_i \text{ for the fluid}, \tag{10}$$

and

$$\frac{\partial (\rho u_j u_i)}{\partial x_j} - \frac{\partial}{\partial x_j}\left[\mu\left(\frac{\partial (\delta u_i)}{\partial x_j} + \frac{\partial (\delta u_j)}{\partial x_i}\right) + \lambda\delta_{ij}\frac{\partial (\delta u_k)}{\partial x_k}\right] = \rho f_i \text{ for the solid}. \tag{11}$$

Equations (10) and (11) can be expressed in terms of a general variable $\phi$ as

$$\frac{\partial (\rho u_j \phi)}{\partial x_j} - \frac{\partial}{\partial x_j}\left[\mu_\phi\left(\frac{\partial \phi}{\partial x_j}\right)\right] = S_\phi, \tag{12}$$

where $S_\phi$ is the source term. The general variable $\phi$ stands for the velocity vector in the fluid and for the displacement vector in the solid. Incompressible flow and constant dynamic viscosity are assumed for the fluid. The source terms are expressed as

$$S_\phi = \rho f_i - \frac{\partial p}{\partial x_i} \text{ for the fluid}, \tag{13}$$

and

$$S_\phi = \rho f_i + \frac{\partial}{\partial x_j}\left[\mu\left(\frac{\partial (\delta u_j)}{\partial x_i}\right) + \lambda\delta_{ij}\frac{\partial (\delta u_k)}{\partial x_k}\right] \text{ for the solid}. \tag{14}$$

The continuity equation, i.e., (1) is redundant and need not be considered for the solid as an elastic solid is assumed. Also it is reasonable to assume for most of the applications in practice that the strains, displacements, velocities and the accelerations are very small. Hence the convective terms are neglected in the solid.

The convective and diffusive terms in the transport equation (12) are discretized using the procedure proposed by Date [3]. This procedure uses the SIMPLE algorithm of Patankar [4] for calculating the velocity and the pressure fields and the smoothing pressure correction algorithm proposed by Date [5] for velocity-pressure coupling. Discretization of the additional terms appearing in the source term for the solid is explained here. The present procedure is an extension of the procedure proposed by Date [3] for solving fluid flow problems. Only the additional work is reported here. Integrating the source term over an arbitrary control volume (CV) or cell, we get

$$\int_{\triangle V} (S_\phi)\, dV = \int_{\triangle V} (\rho f_i)\, dV + \int_{\triangle V}\left[\frac{\partial}{\partial x_j}\left[\mu\left(\frac{\partial (\delta u_j)}{\partial x_i}\right) + \lambda\delta_{ij}\frac{\partial (\delta u_k)}{\partial x_k}\right]\right] dV, \tag{15}$$

where $\triangle V$ is the volume of the CV. The volume integral of the body force is expressed assuming an averaged value of this term stored at the centroid of the CV. To express the volume integrals of the remaining terms Gauss' theorem is used. The volume integrals are converted to the surface integrals to get

$$\int_{\triangle V} (S_\phi)\, dV = \rho f_i \triangle V + \int_S\left[\mu\left(\frac{\partial (\delta u_j)}{\partial x_i}\right) + \lambda\delta_{ij}\frac{\partial (\delta u_k)}{\partial x_k}\right]\cdot dS, \tag{16}$$

where $S$ represents the surface area of the CV. The surface area consists of the CV faces. The surface integrals in (16) are approximated by summations over the CV faces. The flux through a CV face is assumed as an averaged value over the face passing through the face center. Therefore, we get

$$\int_{\triangle V} (S_\phi)\, dV = \rho f_i \triangle V +$$

$$\sum_{k=1}^{Nk}\left[\mu\left(\frac{\partial\left(\delta u_j\right)}{\partial x_i}\right)+\lambda\delta_{ij}\frac{\partial\left(\delta u_k\right)}{\partial x_k}\right]_{ck} n_{jck}A_{fk}, \quad (17)$$

where $k$ on the summation sign represent the $k^{th}$ CV face, $Nk$ is the number of faces enclosing the CV, $n_{jck}$ is the unit outward facing normal to the $k^{th}$ face, with subscript $ck$ representing the face center of the $k^{th}$ face. $A_{fk}$ represents the area of the $k^{th}$ face. Equation (17) is rearranged as

$$\int_{\triangle V}\left(S_\phi\right)dV=\rho f_i\triangle V+\sum_{k=1}^{Nk}\left[\mu\left(\frac{\partial\left(\delta u_j\right)}{\partial x_i}\right)n_j\right]_{ck}A_{fk}+$$

$$\sum_{k=1}^{Nk}\left[\lambda\frac{\partial\left(\delta u_k\right)}{\partial x_k}n_i\right]_{ck}A_{fk}. \quad (18)$$

The displacement gradients at the face center in (18) are calculated assuming a curvilinear coordinate system for each CV face locally. Consider a CV face ABC common between two tetrahedral CVs ABCD and ABCF as shown in Fig. 1. For this face the local coordinate system consists of the directions $\xi_1$ along the line joining the adjacent CV centers P and E and $\xi_2$ and $\xi_3$ along two of the sides of the face, say CA and CB respectively. Then using the coordinate transformation between the local curvilinear coordinates $\xi_j$ and the global cartesian coordinates $x_j$, we have

$$\frac{\partial\left(\delta u_i\right)}{\partial x_i}=\frac{1}{J}\left[\beta_j^i\frac{\partial\left(\delta u_i\right)}{\partial\xi_j}\right], \quad (19)$$

where $J$ stands for the Jacobian of the matrix evolving during the transformation process. It is expressed as

$$J=\frac{\partial x_1}{\partial\xi_j}\beta_j^1. \quad (20)$$

The geometric coefficients $\beta_j^i$ are expressed as

$$\beta_j^i=\frac{\partial x_p}{\partial\xi_r}\frac{\partial x_q}{\partial\xi_s}-\frac{\partial x_q}{\partial\xi_r}\frac{\partial x_p}{\partial\xi_s}, \quad (21)$$

where $i,p,q$ are cyclic and $j,r,s$ are cyclic.

Consider again the CV face ABC common between the two tetrahedral CVs ABCD and ABCF as shown in Fig. 1. The gradients of displacements with respect to the local coordinates $\xi_j$ in (19) are expressed as

$$\frac{\partial\left(\delta u_i\right)}{\partial\xi_1}=\frac{\delta u_{i,E}-\delta u_{i,P}}{l_{PE}}, \quad (22)$$

$$\frac{\partial\left(\delta u_i\right)}{\partial\xi_2}=\frac{\delta u_{i,A}-\delta u_{i,C}}{l_{AC}}, \quad (23)$$

and

$$\frac{\partial\left(\delta u_i\right)}{\partial\xi_3}=\frac{\delta u_{i,B}-\delta u_{i,C}}{l_{BC}}, \quad (24)$$

where $\delta u_i$ is the $i^{th}$ component of the displacement vector $\delta u_j$. $l$ stands for the length. The $\delta u_i$ at the face vertices A, B and C in (22), (23) and (24) are expressed in terms of the values at the CV centers P and E assuming linear variation in the neighbourhood of the nodes P and E. For example, at the vertex A

$$\delta u_{i,A}=\frac{1}{2}\left[\delta u_{i,P}+\left(\frac{\partial\left(\delta u_i\right)}{\partial x_j}\right)_P\left(x_{j,A}-x_{j,P}\right)\right]+$$

$$\frac{1}{2}\left[\delta u_{i,E}+\left(\frac{\partial\left(\delta u_i\right)}{\partial x_j}\right)_E\left(x_{j,A}-x_{j,E}\right)\right]. \quad (25)$$

The gradients $\partial\left(\delta u_i\right)/\partial x_j$ at the CV centers P and E in (25) are calculated using the method of least squares [1].

There are three type of boundary conditions possible for the solid region. They are:

(i) The displacement vector is prescribed (Dirichlet type boundary condition). This is expressed as

$$\delta u_j\left(r_j\right)=\delta u_{j,B},\ r_j\in S, \quad (26)$$

where $r_j$ is the position vector, $\delta u_{j,B}$ is the prescribed displacement vector at the boundary and $S$ is the boundary surface. When the displacement vector is known at the boundaries it is directly substituted into the discretized governing equations.

(ii) The forces per unit area vector or traction vector is prescribed (Neumann type boundary condition). Mathematically this is written as

$$t_j\left(r_j\right)=t_{j,B},\ r_j\in S, \quad (27)$$

where $t_j$ is the traction vector and $t_{j,B}$ is the prescribed traction vector at the boundary. The boundary on which the traction condition is known is excluded from the discretization process. The traction vector acting on the boundary is used to calculate the force vector acting on the boundary which is then added to the source term.

(iii) The boundary lies on the plane of symmetry of the domain (Symmetry boundary condition). For this boundary condition the information known is

$$\delta u_n=0,\quad \frac{\partial\delta u_t}{\partial n}=0, \quad (28)$$

where $n$ is the normal to the symmetry plane. $\delta u_n$ and $\delta u_t$ are the displacement components in the normal and tangential directions to the symmetry plane respectively. When symmetry condition is known the displacement vector at the boundary is calculated from (28). Then it becomes Dirichlet type of boundary condition.

## III. Solution procedure

The solution domain is discretized by mapping the whole solution domain comprising of the fluid flow and the solid with a mesh consisting of a finite number of contiguous CVs. The mesh generation is carried out using an educational version of the commercial code ANSYS$^{\mathrm{TM}}$. The number of CVs in the fluid region is $\mathrm{N_f}$. Hence, there are $\mathrm{N_f}$ linear equations obtained by discretization of the governing equations for each variable (pressure and three velocity components) in the fluid region. The set of linear equations for each variable is

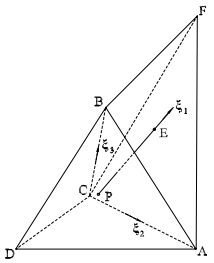


Fig. 1: Local coordinate system

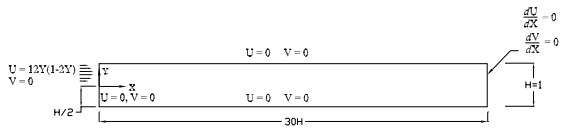


Fig. 2: Computational domain for flow over a backward facing step

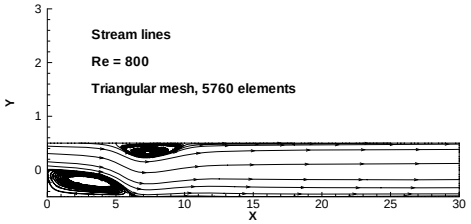


Fig. 3: Streamlines for flow over a backward facing step

solved using the point-by-point Gauss-Seidel algorithm. The converged solution is assumed when the mass and momentum residuals are reduced below $10^{-5}$ for each CV . The pressure field obtained from the flow solution is used as one of the boundary conditions for the solid. Now the displacement field in the solid is calculated. For that the three components of the displacement vector along the three coordinate directions need to be determined. There are $\mathrm{N_s}$ linear equations obtained by discretization of the governing equations for each variable in the solid region, where $\mathrm{N_s}$ is the number of CVs in the solid region. This set of linear equations is solved using the point-by-point Gauss-Seidel algorithm. When the residuals are reduced below $10^{-3}$ for each CV, the converged solution is assumed. Once the displacement field is known the stress field is calculated using the constitutive relation (6) and the kinematic relation (9).

## IV. Validation of the Procedure

To validate the discretization procedure proposed here two benchmark problems are solved, one from fluid mechanics and another from solid mechanics. They are described below.

### A. Flow over a backward facing step

As shown in Fig. 2, the computational domain consists of a rectangular region of height H and length 30H. At the beginning of this region a step of height $\mathrm{H}/2$ is provided. A fully developed flow enters the region through the inlet of height $\mathrm{H}/2$ above the step. Both velocity components are zero on all solid walls including the step. It is assumed that the flow becomes fully developed at the exit as sufficient length of the channel is considered. Normal gradient of all dependent variables is set equal to zero at the exit. A standard test case of Reynolds number (Re) equal to 800 is considered. The Reynolds number is based on the height H and the mean velocity of the fluid at the inlet $\bar{u}_{in}$. The dimension-less form of the governing equations is used to solve the problem. The dimension-less coordinates X and Y are obtained by dividing the dimensional coordinates x and y respectively by H. To obtain the dimension-less x and y velocities, i.e., U and V, the dimensional velocities u and v are divided by $\bar{u}_{in}$. Central Difference Scheme (CDS) dominating blend (0.9 CDS ) of Upwind Difference Scheme (UDS) and Central Difference Scheme is used as the advection scheme. CDS is used for the diffusion terms. The flow streamlines are shown in Fig. 3.

The flow entering above the step separates from the lower wall / step-wall downstream of the step. The flow then re-attaches to the lower wall at a length of approximately 6H. This forms a recirculation zone in the step corner. The length of this zone is calculated to be 6.03 using the present procedure as against 5.94 obtained by Karki et al. [6]. Due to sudden expansion at the inlet, the pressure of the fluid decreases. Recovery of the pressure takes place along the downstream up to a certain length. In this region, separation of the flow from the upper / no step-wall is also seen due to adverse pressure gradient. Further downstream, the flow reattaches. This forms another recirculation zone. The length of this zone is calculated as 5.53; it is equal to 5.51 reported by Karki et al. [6]. The x-velocity profiles in the sections at different axial locations are shown in Fig. 4. The results are found to be in good agreement with that of Karki et al. [6].

### B. Flat plate with a circular hole subjected to uniform tension

A case of an infinite flat plate with a small circular hole in its center and subjected to a uniform tension in one direction is considered. The schematic of the model is shown in Fig. 5. For this problem an analytical solution is available [7]. To solve the problem, finite dimensions of the plate are considered such that the hole is still considered to be small. One quarter of the domain, i.e., ABCDE is used due to symmetry. At the top and right edges, CD and BC respectively, of the domain the stresses obtained using the analytical solution are used as the boundary condition. Symmetry boundary condition is used at the left and bottom edges, i.e., at DE and AB respectively. The value used of the uniform tension $t_x$ in the x-direction is $10^4$ Pa. The material properties assumed are E=$10^7$ Pa and $\upsilon = 0.3$. Figure 6 shows the overlapping plots of the stresses in the plate calculated using the present procedure and that obtained

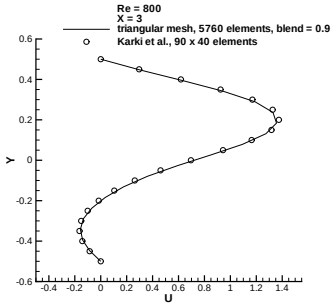


(a) X = 3

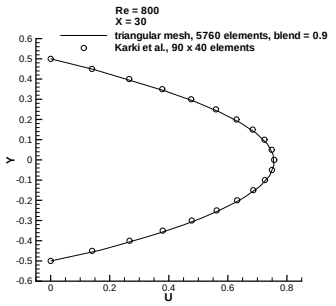


(b) X = 30

Fig. 4: The x-velocity profiles for flow over a backward facing step

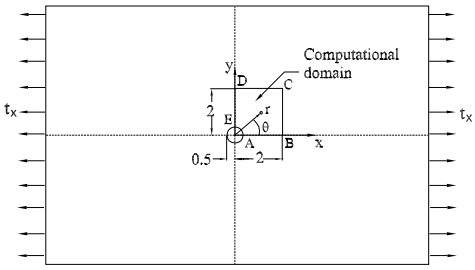


Fig. 5: Schematic of the model problem for stress analysis

using the analytical solutions. Good agreement between the two is seen.

## V. Flow through a U-shaped channel embedded in a plate and the resultant stresses in the plate

The schematic of the model is shown in Fig. 7. Flow of a fluid through an eccentric plane channel embedded in a plate is considered. Due to the fluid pressure forces acting on the channel walls, a displacement field is set up in the plate. It is assumed that the plate is clamped on the outer periphery. Hence, a stress field is also set up in the plate. The flow field in the channel is calculated and the displacement field and the stress field in the plate are calculated. Water ($\rho = 1000\, kg/m^3,\ \mu = 7.69 \times 10^{-4}\, Pa - s$) is considered as the fluid. Aluminum ($E = 6.9 \times 10^{10},\ \upsilon = 0.33$) is selected

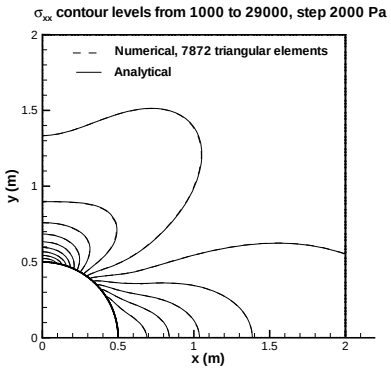


(a) $\sigma_{xx}$

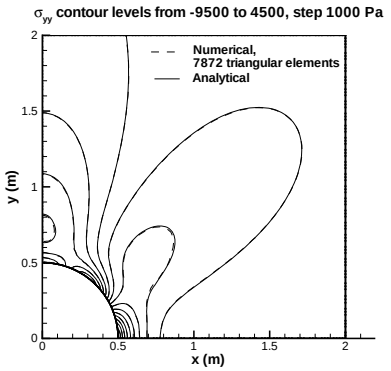


(b) $\sigma_{yy}$

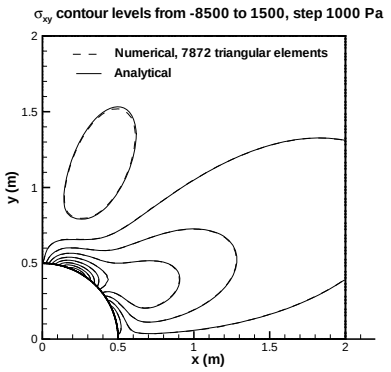


(c) $\sigma_{xy}$

Fig. 6: Stress fields for the model problem for stress analysis

as the plate material. It is assumed that the water enters the channel with a velocity of 1 $m/s$. The pressure of water equal to zero is assumed at the exit. The channel hydraulic diameter is 2 mm. The flow Reynolds number is equivalent to 2600. The assumption that the flow is two-dimensional implies that the plate is thick. Hence, plane strain assumption is used for calculating the displacements and the stresses in the plate.

The mesh used is shown in Fig. 8. The contours of the fluid pressure are shown in Fig.9. Figure 10 shows profiles of

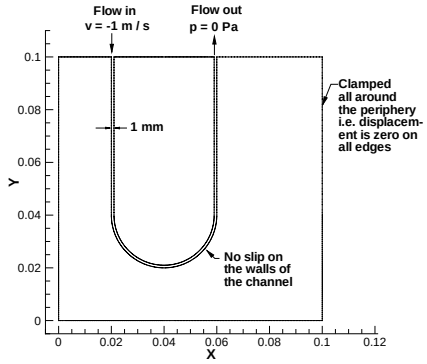


Fig. 7: Schematic of the U-shaped channel problem

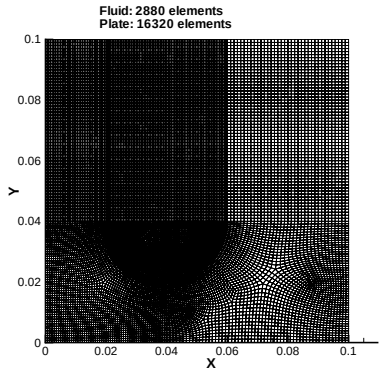


Fig. 8: Mesh used for the U-shaped channel problem

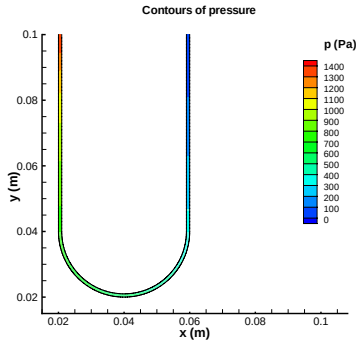


Fig. 9: Pressure contours for the U-shaped channel problem

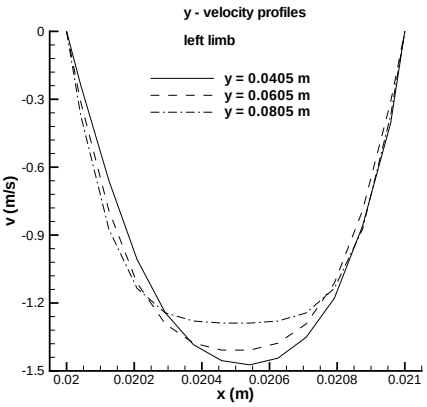


(a) Left limb

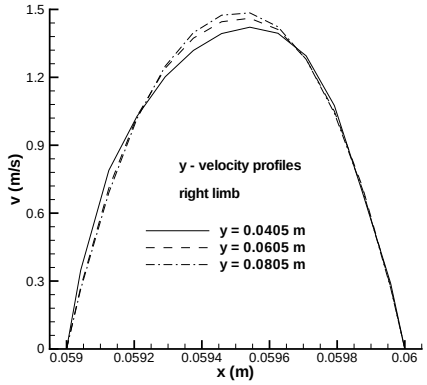


(b) Right limb

Fig. 10: y-velocity profiles for the U-shaped channel problem

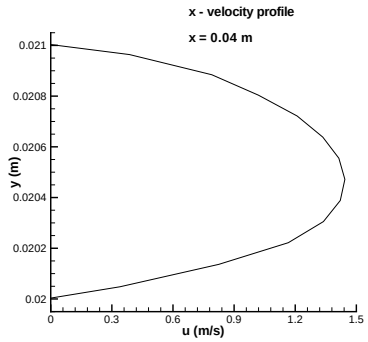


Fig. 11: x-velocity profile in a vertical section through the lowermost point of the Ushaped channel

y-velocity in a few horizontal sections at different locations along the flow. In Fig. 11 the x-velocity profile is shown in the vertical section through the lowermost point of the channel. The displacement contours are shown in Fig. 12. It is seen that the portion of the plate circumscribed by the channel experiences larger displacements. Since the pressure of the fluid in the left limb of the channel is higher than that in the right limb, this portion of the plate is subjected to a net force in the positive x-direction. Consequently, the x-displacements are positive. Also, since this portion is clamped at the top edge, the x-displacements increase from the clamped edge towards the channel bend. In addition, this portion is also subjected to a compressive force due to the fluid pressure in the left and right limbs of the channel. This causes the material within this portion to move along the limbs constituting the y-

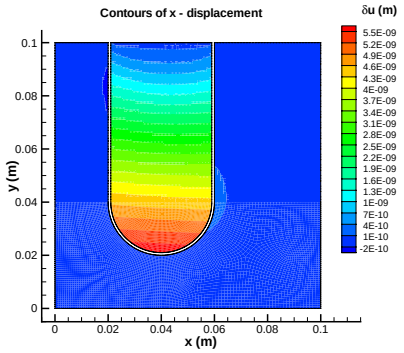


(a) x-displacements

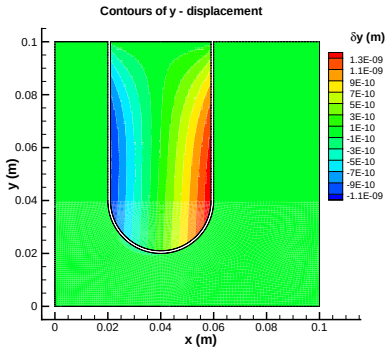


(b) y-displacement

Fig. 12: Displacement contours for the U-shaped channel problem

displacements. The y-displacements are negative near the left limb and are positive near the right limb. This is due to the combined effect of the pressure forces in the left limb, in the bend, in the right limb and zero displacement at the top edge. The contours of the stress fields are shown in Fig. 13. It is seen that $\sigma_{xx}$ is larger near the left limb than near the right limb due to the fluid pressure being higher in the left limb. The stresses are maximum in the region of the plate near the inlet and the outlet where the displacements are minimum. The behaviour of the stresses is consistent with that of the displacements.

## VI. Conclusions

A co-located finite volume procedure is developed for the solution of fluid-structure interaction type of problems. The procedure is validated by solving a few benchmark problems and comparing the results with those available in the literature. Two-dimensional cases are presented for simplicity. A fluid structure interaction problem is solved wherein the flow of a fluid through an eccentric U-shaped plane channel embedded in a plate is considered. The resulting stress and displacement fields in the plate are analyzed and found to be qualitatively correct based on physical grounds.

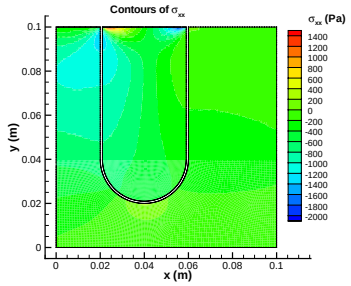


(a) $\sigma_{xx}$

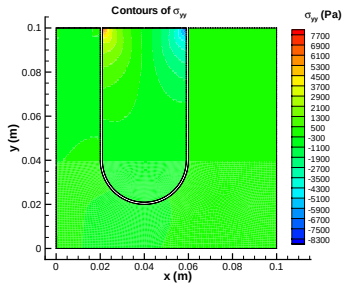


(b) $\sigma_{yy}$

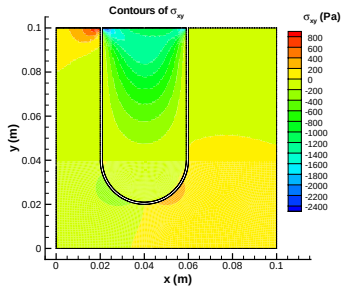


(c) $\sigma_{xy}$

Fig. 13: Stress contours for the U-shaped channel problem

## References

[1] I. Demirdzic and S. Muzaferija, “Numerical method for coupled fluid flow, heat transfer and stress analysis using unstructured moving meshes with cells of arbitrary topology”, *Comput. Methods Appl. Mech. Engrg.*, vol. 125, pp. 235-255, 1995.

[2] Michael Schafer and Ilka Teschauer, “Numerical simulation of coupled fluid-solid problems”, *Comput. Methods Appl. Mech. Engrg.*, vol. 190, pp. 3645-3667, 2001.

[3] A. W. Date, “Solution of transport equations on unstructured meshes with cell-centered colocated variables: Part I: Discretization, *International Journal of Heat and Mass Transfer*, vol. 48, pp. 1117-1127, 2005.

[4] S. V. Patankar, *Numerical Heat Transfer and Fluid Flow*, Hemisphere Publishing Corp.: New York, 1980, ch. 6.

[5] A.W. Date, “Fluid dynamical view of pressure checkerboarding problem and smoothing pressure correction on meshes with colocated variables”, *International Journal of Heat and Mass Transfer*, vol. 46, pp. 4885–4898, 2003.

[6] K. C. Karki, K. M. Kelkar, P. S. Sathyamurthy and S. V. Patankar, “Accurate solutions for laminar flow and heat transfer in a channel with a backward-facing step, benchmark problems for heat transfer codes”, *ASME HTD*, vol. 222, pp. 35-43, 1992.

[7] I. Demirdzic, S. Muzaferija and M. Peric, “Benchmark solutions of some structural analysis problems using finite-volume method and multigrid acceleration”, *International Journal for Numerical Methods in Engineering*, vol. 40, pp. 1893-1908, 1997.